Modeling of Damage Evolution in Particulate Reinforced Composites with VCFEM

Ran Guo[1,*], Wenyan Zhang[1], Benning Qu[1], Yongjin Chen[1]

[1] Department of Engineering Mechanics, Faculty of Civil Engineering and Architecture, Kunming University of Science and Technology, Kunming 650500, China
[2] Faculty of EEFF, Institute of GGHH, City Post Code, Country
* Corresponding author: prof.guo@189.cn

Abstract The modeling of fatigue crack initiation and propagation for particulate reinforced composites and the study of the behavior of a functionally graded material with interface cracks are facilitated with a new Voronoi Cell Finite Element Method (VCFEM), considering the matrix-inclusion interfacial fatigue crack and matrix fatigue crack. In the new element, all possible contacts on the crack edge are considered by contact seeking and remeshing methods, when the crack is closing under all possible changing loads. The fatigue crack initiates when the fatigue damage exceeds certain critical damage value, and fatigue crack propagation are simulated by gradual seeking crack propagating directions and new crack tips, using a remeshing method that a damaged node at the crack tip is replaced by a pair of nodes, a new crack tip node is assigned at the crack propagating directions and a more pair of nodes are needed to be added on the crack edge near the crack tip in order to better facilitate the free-traction boundary condition. The first example has been given for Particle-reinforced metal-matrix composites with 20 elliptical inclusions to simulate the fatigue crack initiation and propagation under plane stress conditions. It appears that this method is a more efficient way to deal with the interfacial damage of composite materials. In the second example, the results show that the mechanical properties of functionally gradient materials are influenced by the particles' size, topological structure, and interfacial deboning strength. With the interface cracking the overall stiffness of functionally gradient materials is gradually reduced.

Keywords VCFEM, Finite element method, Fatigue crack, Particulate reinforced composites

1. Introduction

Particulate-reinforced metal-matrix composites (MMCs) have attracted significant attention in recent times in both the academic community and in the industrial sector. Since MMC combine well-known superior properties such as low density, high strength, stiffness, creep and wear resistance, they are appropriate candidates for numerous aerospace and automotive applications. However, the differences in thermo-mechanical properties of matrix and inclusion develop stresses during fabrication and in service. This may lead to voids nucleation, cracking and decohesion at the interface, which affects seriously fracture properties.

The validity of modeling real composites practically with heterogeneities of arbitrary shapes, sizes or dispersions, depends considerably on the consideration of the irregular microstructure. The accurate micromechanical modeling of actual two-phase materials is very complicated due to the irregular microstructural configurations that exist in real materials.

A large number of models have been developed to predict the effective elastic properties of heterogeneous materials and their dependence on materials microstructure, such as homogenization theory, cell methods, traditional displacement based FEM, A hybrid finite element approach by Zhang and Katsube[1], a Voronoi Cell Finite Element Method (VCFEM) for modeling of non-uniform microstructures with heterogeneities introduced by Ghosh and co-workers in a series of papers[2~3] and a series of works on VCFEM are done[5-6].

Introduction a new Voronoi cell finite element model (VCFEM) on the base of the assumed stress hybrid variational principle to model fatigue crack initiation and propagation in a Particle-reinforced metal-matrix composites (MMCs) with heterogeneities of arbitrary shapes, sizes or dispersions is the objective of the present study. In the new element, considering the

matrix-inclusion interfacial fatigue crack, matrix fatigue crack and all possible contact on the crack edge, fatigue crack initiation and propagation is simulated by a new remeshing method. All possible contact on the crack edge when the crack closed under all possible fatigue loads are sought along every crack edge. The fatigue crack initiates when the fatigue damage exceeds certain critical damage value. The fatigue crack propagation is simulated by gradually seeking crack propagating directions and new crack tips, using a remeshing method that a damaged node at the crack tip is replaced by a pair of nodes, a new crack tip node is assigned at the crack propagating directions and a more pair of nodes are needed to be added on the crack edge near the new crack tip in order to better facilitate the free-traction boundary condition. The first example has been given for Particle-reinforced metal-matrix composites with 20 elliptical inclusions to simulate the fatigue crack initiation and propagation under plane stress conditions. It appears that this method is a more efficient way to deal with the interfacial damage of composite materials. The simulation results are compared with those of general fine finite element model and a good agreement is obtained. In the second example, the results show that the mechanical properties of functionally gradient materials are influenced by the particles' size, topological structure, and interfacial deboning strength. With the interface cracking the overall stiffness of functionally gradient materials is gradually reduced.

2. The Voronoi Cell Finite Element Model

2.1. Hybrid Element Assumptions and Weak Forms

In the Voronoi cell element method, each cell represents a basic structural element of the microstructure, which includes a particulate with its matrix neighborhood. A new cell element, including an interfacial crack and a matrix crack, is shown in Fig. 1. The matrix and inclusion phase in each Voronoi cell Ω_e are denoted by Ω_m and Ω_c, respectively, i.e., $\Omega_e = \Omega_m \cup \Omega_c$. The bonded inclusion-matrix interface is indicated by $\partial\Omega_b$ and the debonded interface is indicated by $\partial\Omega_c$ on the inclusion side and by $\partial\Omega_m$ on the matrix side. The element boundary $\partial\Omega_e$ is assumed to be composed of prescribed displacement boundary $\partial\Omega_e^d$, prescribed traction boundary $\partial\Omega_e^t$, inter-element boundary $\partial\Omega_e^i$ and free boundary $\partial\Omega_e^f$, i.e., $\partial\Omega_e = \partial\Omega_e^d \cup \partial\Omega_e^t \cup \partial\Omega_e^i \cup \partial\Omega_e^f$. The matrix crack edges $\partial\Omega_{m1}$, $\partial\Omega_{m2}$, $\partial\Omega_{m3}$ and inclusion crack edge $\partial\Omega_c$ have outward normals $\mathbf{n}^{m1}$, $\mathbf{n}^{m2}$, $\mathbf{n}^{m3}$ and $\mathbf{n}^c$, respectively, while $\mathbf{n}^e$ is the outward normal to the element boundary $\partial\Omega_e$.

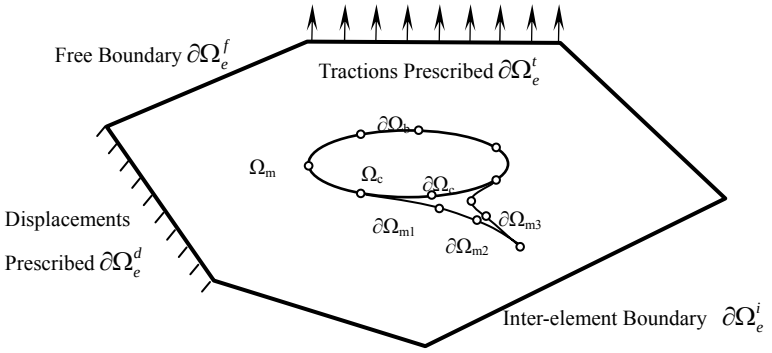

Figure 1. A Voronoi cell finite element with part interfacial crack and matrix crack

In an incremental formulation to account for the onset and growth of the fatigue crack, $\boldsymbol{\sigma}$ is an equilibrated stress field corresponding a strain field $\boldsymbol{\varepsilon}$; $\mathbf{u}$ is a compatible displacement field on the element boundary at the beginning of an increment; $\Delta\boldsymbol{\sigma}$ is the equilibrated stress increment in Ω_e;

$\Delta\mathbf{u}$ is a compatible displacement increment on $\partial\Omega_e$ and $\Delta\bar{\mathbf{f}}$ is a traction increment on the traction boundary $\partial\Omega_e^t$. An element complementary energy function can be expressed as follows:

$$\begin{aligned}
&\Pi_{mc}^{e}\left(\Delta\boldsymbol{\sigma},\Delta\mathbf{u}\right)=\int_{\Omega_e}\frac{1}{2}\left(\boldsymbol{\sigma}+\Delta\boldsymbol{\sigma}\right)\mathbf{S}\left(\boldsymbol{\sigma}+\Delta\boldsymbol{\sigma}\right)d\Omega-\int_{\partial\Omega_e}\mathbf{n}^{e}\cdot\left(\boldsymbol{\sigma}+\Delta\boldsymbol{\sigma}\right)\cdot\left(\mathbf{u}+\Delta\mathbf{u}\right)d\partial\Omega\\
&+\int_{\partial\Omega_{te}}\left(\bar{\mathbf{f}}+\Delta\bar{\mathbf{f}}\right)\cdot\left(\mathbf{u}+\Delta\mathbf{u}\right)d\partial\Omega+\int_{\partial\Omega_b}\mathbf{n}^{b}\cdot\left(\boldsymbol{\sigma}^{m}+\Delta\boldsymbol{\sigma}^{m}-\boldsymbol{\sigma}^{c}-\Delta\boldsymbol{\sigma}^{c}\right)\cdot\left(\mathbf{u}^{b}+\Delta\mathbf{u}^{b}\right)d\partial\Omega\\
&-\int_{\partial\Omega_{m1}}\mathbf{n}^{m1}\cdot\left(\boldsymbol{\sigma}^{m1}+\Delta\boldsymbol{\sigma}^{m1}\right)\cdot\left(\mathbf{u}^{m1}+\Delta\mathbf{u}^{m1}\right)d\partial\Omega-\int_{\partial\Omega_c}\mathbf{n}^{c}\cdot\left(\boldsymbol{\sigma}^{c}+\Delta\boldsymbol{\sigma}^{c}\right)\cdot\left(\mathbf{u}^{c}+\Delta\mathbf{u}^{c}\right)d\partial\Omega\\
&-\int_{\partial\Omega_{m2}}\mathbf{n}^{m2}\cdot\left(\boldsymbol{\sigma}^{m2}+\Delta\boldsymbol{\sigma}^{m2}\right)\cdot\left(\mathbf{u}^{m2}+\Delta\mathbf{u}^{m2}\right)d\partial\Omega\\
&-\int_{\partial\Omega_{m3}}\mathbf{n}^{m3}\cdot\left(\boldsymbol{\sigma}^{m3}+\Delta\boldsymbol{\sigma}^{m3}\right)\cdot\left(\mathbf{u}^{m3}+\Delta\mathbf{u}^{m3}\right)d\partial\Omega
\end{aligned}\tag{1}$$

where, $\Delta\mathbf{u}^{b}$, $\Delta\mathbf{u}^{c}$, $\Delta\mathbf{u}^{m1}$, $\Delta\mathbf{u}^{m2}$ and $\Delta\mathbf{u}^{m3}$ are the displacement increments of the crack edges in an element. The total energy for an entire heterogeneous structure that contains *N* inclusions is obtained by adding the element energy functions for *N* elements:

$$\Pi_{total}^{mc}=\sum_{e=1}^{N}\Pi_{element}^{mc}\tag{2}$$

By setting the first variation of $\Pi_{element}^{mc}$ in Eq.(1) with respect to the stress increments $\Delta\boldsymbol{\sigma}$ to zero, the element displacement relations in each of the element Ω_e can be obtained. Setting the first variation of $\Pi_{element}^{mc}$ with respect to boundary displacement increments $\Delta\mathbf{u}$ to zero, obtains the traction reciprocity conditions on the inter-element boundaries and traction boundaries as shown in Fig. 1, and setting the first variation of $\Pi_{element}^{mc}$ with respect to boundary displacement increments $\Delta\mathbf{u}^{b}$, $\Delta\mathbf{u}^{c}$, $\Delta\mathbf{u}^{m1}$, $\Delta\mathbf{u}^{m2}$ and $\Delta\mathbf{u}^{m3}$ to zero, obtains the traction reciprocity conditions on the interfaces of inclusion-matrix as shown as follows:

$$\begin{aligned}
\mathbf{n}^{b}\cdot\left(\boldsymbol{\sigma}^{c}+\Delta\boldsymbol{\sigma}^{c}\right)&=\mathbf{n}^{b}\cdot\left(\boldsymbol{\sigma}^{m}+\Delta\boldsymbol{\sigma}^{m}\right)\ \text{on bonded interface}\ \partial\Omega_b\\
\mathbf{n}^{c}\cdot\left(\boldsymbol{\sigma}^{c}+\Delta\boldsymbol{\sigma}^{c}\right)&=\mathbf{0}\qquad\text{on debonded interface}\ \partial\Omega_c\\
\mathbf{n}^{m1}\cdot\left(\boldsymbol{\sigma}^{m1}+\Delta\boldsymbol{\sigma}^{m1}\right)&=\mathbf{0}\ \ \text{on debonded interface}\ \partial\Omega_{m1}\\
\mathbf{n}^{m2}\cdot\left(\boldsymbol{\sigma}^{m2}+\Delta\boldsymbol{\sigma}^{m2}\right)&=\mathbf{0}\qquad\text{on the first crack edgee}\ \partial\Omega_{m2}\\
\mathbf{n}^{m3}\cdot\left(\boldsymbol{\sigma}^{m3}+\Delta\boldsymbol{\sigma}^{m3}\right)&=\mathbf{0}\ \ \text{on the second crack edge}\ \ \partial\Omega_{m3}
\end{aligned}\tag{3}$$

2.2. Method of Solution

The stresses in the matrix and inclusion phases can be individually described to accommodate stress jumps across the interface. The expressions may be assumed for stress functions $\Phi(x,y)$ in the matrix and inclusion phases in the form as

$$\Delta\boldsymbol{\sigma}^{m}=\mathbf{P}^{m}\Delta\boldsymbol{\beta}^{m}\qquad(\text{in}\ \ \Omega_m)\tag{4}$$

$$\Delta\boldsymbol{\sigma}^{c}=\mathbf{P}^{c}\Delta\boldsymbol{\beta}^{c}\qquad(\text{in}\ \ \Omega_c)\tag{5}$$

where $\Delta\boldsymbol{\beta}^{m}$ and $\Delta\boldsymbol{\beta}^{c}$ correspond to a set of undetermined stress coefficients; $\mathbf{P}^{m}$ and $\mathbf{P}^{c}$ are matrixes of interpolation functions. Compatible displacement increments on the element boundary $\partial\Omega_e$ as well as on the crack edges $\partial\Omega_b$, $\partial\Omega_c$ and $\partial\Omega_m$ are generated by interpolating in terms of generalized nodal values as:

$$\Delta\mathbf{u}=\mathbf{L}\left\{\Delta\mathbf{q}^{e}\right\},\ on\ \ \partial\Omega_e;$$

$$\Delta\mathbf{u}^b = \mathbf{L}^b\left\{\Delta\mathbf{q}^b\right\},\ on\ \ \partial\Omega_b\ ;$$

$$\Delta\mathbf{u}^c = \mathbf{L}^c\left\{\Delta\mathbf{q}^c\right\},\ on\ \ \partial\Omega_c\ ;$$

$$\Delta\mathbf{u}^{m1} = \mathbf{L}^{m1}\left\{\Delta\mathbf{q}^{m1}\right\},\ \text{on}\ \ \partial\Omega_{m1}\ ; \tag{6}$$

$$\Delta\mathbf{u}^{m2} = \mathbf{L}^{m2}\left\{\Delta\mathbf{q}^{m2}\right\},\ \text{on}\ \ \partial\Omega_{m2}\ ;$$

$$\Delta\mathbf{u}^{m3} = \mathbf{L}^{m3}\left\{\Delta\mathbf{q}^{m3}\right\},\ \text{on}\ \ \partial\Omega_{m3}$$

where $\Delta\mathbf{q}^e$, $\Delta\mathbf{q}^b$, $\Delta\mathbf{q}^{m1}$, $\Delta\mathbf{q}^{m2}$, $\Delta\mathbf{q}^{m3}$ and $\Delta\mathbf{q}^c$ are generalized displacement increment vectors, and $\mathbf{L}$, $\mathbf{L}^b$, $\mathbf{L}^{m1}$, $\mathbf{L}^{m2}$, $\mathbf{L}^{m3}$ and $\mathbf{L}^c$ are interpolation matrices. Substituting Eq. (4), (5) and (6) into the energy function (1), and setting the first variations of $\Pi^{mc}_{element}$ with respect to the stress coefficients $\Delta\boldsymbol{\beta}^m$ and $\Delta\boldsymbol{\beta}^c$, respectively to zero, yields following two weak forms of the kinematic relations. Let $\{d\beta\}^i$ corresponds to the correction to $\Delta\beta$'s in the i^{th} iteration, the weak form of the kinematic relations may be expressed as:

$$\begin{bmatrix}\mathbf{H}^m & \mathbf{0}\\ \mathbf{0} & \mathbf{H}^c\end{bmatrix}\begin{Bmatrix}d\boldsymbol{\beta}^{m^i}\\ d\boldsymbol{\beta}^{c^i}\end{Bmatrix}=\begin{bmatrix}\mathbf{G}_e & -\mathbf{G}_{mb} & \mathbf{G}_{mm1} & \mathbf{0} & \mathbf{G}_{mm2} & \mathbf{G}_{mm3}\\ \mathbf{0} & \mathbf{G}_{cb} & \mathbf{0} & \mathbf{G}_{cc} & \mathbf{0} & \mathbf{0}\end{bmatrix}\begin{Bmatrix}d\mathbf{q}^{e^i}\\ d\mathbf{q}^{b^i}\\ d\mathbf{q}^{m1^i}\\ d\mathbf{q}^{c^i}\\ d\mathbf{q}^{m2^i}\\ d\mathbf{q}^{m3^i}\end{Bmatrix} \tag{7}$$

where

$$\mathbf{H}^m = \int_{\Omega_m}\mathbf{P}^{m^T}\mathbf{S}_m\mathbf{P}^m d\Omega \tag{8}$$

$$\mathbf{H}^c = \int_{\Omega_c}\mathbf{P}^{c^T}\mathbf{S}_c\mathbf{P}^c d\Omega \tag{9}$$

$$\mathbf{G}_e = \int_{\partial\Omega_e}\mathbf{P}^{m^T}\mathbf{n}^{e^T}\mathbf{L}d\partial\Omega \tag{10}$$

$$\mathbf{G}_{mm1} = \int_{\partial\Omega_m}\mathbf{P}^{m^T}\mathbf{n}^{m1^T}\mathbf{L}^{m1}d\partial\Omega \tag{11}$$

$$\mathbf{G}_{mm2} = \int_{\partial\Omega_m}\mathbf{P}^{m^T}\mathbf{n}^{m2^T}\mathbf{L}^{m2}d\partial\Omega \tag{12}$$

$$\mathbf{G}_{mm3} = \int_{\partial\Omega_m}\mathbf{P}^{m^T}\mathbf{n}^{m3^T}\mathbf{L}^{m3}d\partial\Omega \tag{13}$$

$$\mathbf{G}_{cc} = \int_{\partial\Omega_c}\mathbf{P}^{c^T}\mathbf{n}^{c^T}\mathbf{L}^c d\partial\Omega \tag{14}$$

$$\mathbf{G}_{mb} = \int_{\partial\Omega_b}\mathbf{P}^{m^T}\mathbf{n}^{b^T}\mathbf{L}^b d\partial\Omega \tag{15}$$

$$\mathbf{G}_{cb} = \int_{\partial\Omega_b}\mathbf{P}^{c^T}\mathbf{n}^{b^T}\mathbf{L}^b d\partial\Omega \tag{16}$$

or in a condensed form

$$d\boldsymbol{\beta}^i = \mathbf{H}^{-1}\mathbf{G}d\mathbf{q}^i \tag{17}$$

Setting the first variation of the total energy functional (1) with respect to $\Delta\mathbf{q}^e$, $\Delta\mathbf{q}^b$, $\Delta\mathbf{q}^m$ and $\Delta\mathbf{q}^c$ to zero, results in the weak form of the traction reciprocity conditions as

$$\sum_e \mathbf{G}^T d\boldsymbol{\beta}^i = \sum_e \overline{\mathbf{F}} - \sum_e \mathbf{G}^T \begin{Bmatrix} \boldsymbol{\beta}^m + \Delta\boldsymbol{\beta}^{m^i} \\ \boldsymbol{\beta}^c + \Delta\boldsymbol{\beta}^{c^i} \end{Bmatrix} \tag{18}$$

where

$$\overline{\mathbf{F}} = \begin{bmatrix} \overline{\mathbf{F}}^e \\ \mathbf{0} \\ \mathbf{0} \\ \mathbf{0} \\ \mathbf{0} \\ \mathbf{0} \end{bmatrix}; \qquad \overline{\mathbf{F}}^{eT} = \int_{\partial\Omega_{tc}} \left(\overline{\mathbf{f}} + \Delta\overline{\mathbf{f}} \right)^T \mathbf{L} d\partial\Omega \tag{19}$$

Substituting Eq. (17) into the weak form expressions of the traction reciprocity conditions Eq. (18), yields:

$$\sum_e \mathbf{K}_e d\mathbf{q}^i = \sum_e \overline{\mathbf{F}} - \sum_e \mathbf{G}^T \begin{Bmatrix} \boldsymbol{\beta}^m + \Delta\boldsymbol{\beta}^{m^i} \\ \boldsymbol{\beta}^c + \Delta\boldsymbol{\beta}^{c^i} \end{Bmatrix} \tag{20}$$

where

$$\mathbf{K}_e = \begin{bmatrix} \mathbf{G}_e^T & \mathbf{0} \\ -\mathbf{G}_{mb}^T & \mathbf{G}_{cb}^T \\ \mathbf{G}_{mm1}^T & \mathbf{0} \\ \mathbf{0} & \mathbf{G}_{cc}^T \\ \mathbf{G}_{mm2}^T & \mathbf{0} \\ \mathbf{G}_{mm3}^T & \mathbf{0} \end{bmatrix} \cdot \begin{bmatrix} \mathbf{H}^{m^{-1}} & \mathbf{0} \\ \mathbf{0} & \mathbf{H}^{c^{-1}} \end{bmatrix} \cdot \begin{bmatrix} \mathbf{G}_e & -\mathbf{G}_{mb} & \mathbf{G}_{mm1} & \mathbf{0} & \mathbf{G}_{mm2} & \mathbf{G}_{mm3} \\ \mathbf{0} & \mathbf{G}_{cb} & \mathbf{0} & \mathbf{G}_{cc} & \mathbf{0} & \mathbf{0} \end{bmatrix} = \begin{bmatrix} \mathbf{K}_1 & \mathbf{K}_2 \end{bmatrix} \tag{21}$$

$$\mathbf{K}_1 = \begin{bmatrix} \mathbf{G}_e^T \mathbf{H}^{m^{-1}} \mathbf{G}_e & -\mathbf{G}_e^T \mathbf{H}^{m^{-1}} \mathbf{G}_{mb} & \mathbf{G}_e^T \mathbf{H}^{m^{-1}} \mathbf{G}_{mm1} \\ -\mathbf{G}_{mb}^T \mathbf{H}^{m^{-1}} \mathbf{G}_e & \mathbf{G}_{mb}^T \mathbf{H}^{m^{-1}} \mathbf{G}_{mb} + \mathbf{G}_{cb}^T \mathbf{H}^{c^{-1}} \mathbf{G}_{cb} & -\mathbf{G}_{mb}^T \mathbf{H}^{m^{-1}} \mathbf{G}_{mm1} \\ \mathbf{G}_{mm1}^T \mathbf{H}^{m^{-1}} \mathbf{G}_e & -\mathbf{G}_{mm1}^T \mathbf{H}^{m^{-1}} \mathbf{G}_{mb} & \mathbf{G}_{mm1}^T \mathbf{H}^{m^{-1}} \mathbf{G}_{mm1} \\ \mathbf{0} & \mathbf{G}_{cc}^T \mathbf{H}^{c^{-1}} \mathbf{G}_{cb} & \mathbf{0} \\ \mathbf{G}_{mm2}^T \mathbf{H}^{m^{-1}} \mathbf{G}_e & -\mathbf{G}_{mm2}^T \mathbf{H}^{m^{-1}} \mathbf{G}_{mb} & \mathbf{G}_{mm2}^T \mathbf{H}^{m^{-1}} \mathbf{G}_{mm1} \\ \mathbf{G}_{mm3}^T \mathbf{H}^{m^{-1}} \mathbf{G}_e & -\mathbf{G}_{mm3}^T \mathbf{H}^{m^{-1}} \mathbf{G}_{mb} & \mathbf{G}_{mm3}^T \mathbf{H}^{m^{-1}} \mathbf{G}_{mm1} \end{bmatrix} \mathbf{K}_2 = \begin{bmatrix} \mathbf{0} & \mathbf{G}_e^T \mathbf{H}^{m^{-1}} \mathbf{G}_{mm2} & \mathbf{G}_e^T \mathbf{H}^{m^{-1}} \mathbf{G}_{mm3} \\ \mathbf{G}_{cb}^T \mathbf{H}^{c^{-1}} \mathbf{G}_{cc} & -\mathbf{G}_{mb}^T \mathbf{H}^{m^{-1}} \mathbf{G}_{mm2} & -\mathbf{G}_{mb}^T \mathbf{H}^{m^{-1}} \mathbf{G}_{mm3} \\ \mathbf{0} & \mathbf{G}_{mm1}^T \mathbf{H}^{m^{-1}} \mathbf{G}_{mm2} & \mathbf{G}_{mm1}^T \mathbf{H}^{m^{-1}} \mathbf{G}_{mm3} \\ \mathbf{G}_{cc}^T \mathbf{H}^{c^{-1}} \mathbf{G}_{cc} & \mathbf{0} & \mathbf{0} \\ \mathbf{0} & \mathbf{G}_{mm2}^T \mathbf{H}^{m^{-1}} \mathbf{G}_{mm2} & \mathbf{G}_{mm2}^T \mathbf{H}^{m^{-1}} \mathbf{G}_{mm3} \\ \mathbf{0} & \mathbf{G}_{mm3}^T \mathbf{H}^{m^{-1}} \mathbf{G}_{mm2} & \mathbf{G}_{mm3}^T \mathbf{H}^{m^{-1}} \mathbf{G}_{mm3} \end{bmatrix}$$

Eq. (21) is used to iteratively calculate for the nodal displacement increments. Then, the stress coefficients may be calculated by Eq. (17) and the stresses at any location within the element may be obtained from (4) and (5).

2.3. Simulation of Fatigue Crack Initiation and Propagation

Under the constant amplitude loadings, the fatigue damage under a non-linear fatigue damage rule evolutes as:

$$\frac{\delta\omega}{\delta N} = [\frac{\Delta\sigma}{2B(1-\omega)}]^{\beta} (1-\omega)^{-\gamma} \tag{22}$$

where B，β and γ are the material constants. Eq. (22) deduces the fatigue life:

$$N_F(\Delta\sigma, \overline{\sigma}) = \frac{1}{\beta+\gamma+1} [\frac{\Delta\sigma}{2B(\overline{\sigma})}] \tag{23}$$

For simulating fatigue damage accumulation under gradual step-by-step constant amplitude loadings, the fatigue damage accumulation at the n^{th} step is deduced by integrating Eq. (22).

$$\omega_n = 1-[(1-\omega_{n-1})^m - mN_n(\frac{\Delta\sigma_n}{2B})^\beta]^{\frac{1}{m}} \quad (24)$$

where where ω_{n-1} is the total fatigue damage at the end of the n-1th step; N_n is the cycle life increment at the nth step; $\Delta\sigma_n$ is the nth constant amplitude loading ; the variable $m = 1+\gamma+\beta$; the material constants $B = b_1 + b_2\overline{\sigma}_n$; b_1 and b_2 are the material constants.

3. Examples of Numerical Calculation

All analyses of numerical examples conducted with the VCFEM codes are executed under plane stress assumptions.

3.1. Simulation of the Damage in Complex Microstructure

In the first example, a structure consists of 20 elliptical inclusions with different size (see Fig. 2a). The inclusions are arranged randomly in a square matrix of 10×10 mm^2 and the matrix-inclusion interface of every inclusion is composed of 8 sides, in which no side is debonded before loading. The fatigue crack will initiate and propagate gradually where the total fatigue damage of the interfacial points is greater than the given critical fatigue damage. The vertical displacement on the top edge and the bottom edge and the horizontal displacement on the left edge are fixed, and the displacement controlled fatigue loads are applied on the right edge with the maximal displacement 7×10^{-6} mm and the minimal displacement 7×10^{-7} mm.

Figure 2. (a) The crack propagation status in a square particulate reinforced composites plate with 20 circle inclusions; (b) the horizontal stress component contours within the matrix and inclusion of VCFEM model

Material properties are as follows:
Matrix(Al2024): Young's Modulus $E_{Al} = 72\ GPa$, Poisson's Ratio $v_{Al} = 0.33$;
Inclusions(SiC): Young's Modulus $E_{SiC} = 430\ GPa$, Poisson's Ratio $v_{SiC} = 0.25$;

The given critical fatigue damage c=1 and the material constant β=6， m=1.

In every VCFEM element the stress field in the matrix is represented by a 75 terms expansion composed of 42 polynomial terms (8th order complete polynomial expansion of the Airy function) and 33 reciprocal terms (1 reciprocal terms for each exponent in the polynomial terms, from 2 to 7) While the stress field in the inclusions is modeled using only the first 63 polynomial terms. The

fatigue crack propagation status is shown in Fig. 2(a), and the distribution of the horizontal stress component σ_x calculated by the VCFEM model is showed in Fig. 2(b), when fatigue cycles are 8×10^5. It appears that the VCFEM model has considerable accuracy and high efficiency in dealing with the initiation and propagation of the fatigue crack of Particle-reinforced metal-matrix composites.

3.2. The Study of the Behaviour of a Functionally Graded Material

In the second example, the fatigue crack evolution in the SiC/Al functionally gradient material are simulated with the different volume fraction ratio of SiC of 25%, 40%, 55%, 70%, in which the specific distribution is shown in Fig. 3(a) and the specify voronoi tessellation mesh of functionally gradient materials is shown in Fig. 3(b).

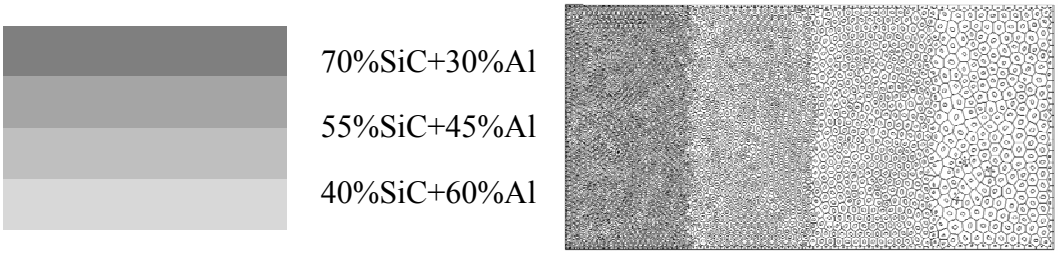

Figure 3. (a) section schematic of SiC/Al functionally gradient materials;
(b) Voronoi tessellation mesh of FGMS

In this model, the Al is Al2024-T6 with the elastic modulus E_{Al} = 72GPa; the Poisson's ratio V_{Al} = 0.33; the yield stress was 70MPa; tangent modulus E_t = 14.5GPa; followed J2 flow theory; SiC is with the elastic modulus E_{SiC} = 430GPa; Poisson's ratio V_{SiC} = 0.25; the yield stress of SiC 100MPa; tangent modulus 50GPa. The width of the specimen is 4mm; the thickness is 8mm, each gradient layer thickness is 2mm. About 4700 inclusions were modeled, the boundary conditions of the model were constrained as follows: the right hands of this specimen were constrained in Ux, Uy directions, and the left hands of the specimen were enforced 0.001 uniform displacement. The critical normal stress leading interfacial crack is 30MPa. In order to evaluate the influence of the interface cracks, a comparison with the model which does not take the interface cracks into consideration was made. The curve of displacement and reaction force was shown in Fig. 4.

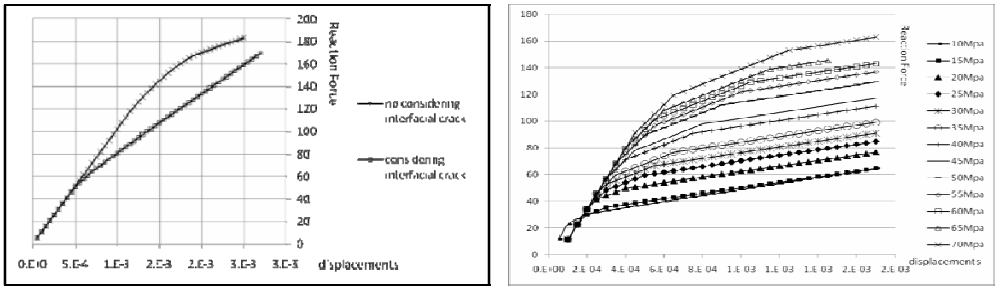

Figure 4. (a) curves of displacement and reaction force;
(b) The effect of interface bond strength

In Fig. 4(a), the results show that the overall stiffness of functionally gradient materials is gradually reduced when the interfaces are cracked. Compared with the model which does not take the interface cracks into consideration the overall stiffness is reduced largely. In Fig. 4(b), the results show that the overall stiffness of the specimen is increasing with the enhancement of interface bond strength. In this test, we can see that when the interface bond strength is between 10-35MPa the overall stiffness of the specimen is increased slowly or can't even reach the yield strength. In this case the SiC particles are a kind of damage to the Al matrixes, because they cannot work together

perfectly. With interface bond strength increasing for example between 35-70MPa, the overall stiffness of the specimen is increased obviously. And the yield strength is higher than 90MPa. So in this situation the spacemen can work very well. And the gradient performance of the functionally gradient materials is not obviously affected by the interfacial crack.

4. Conclusion

In this study, the modeling of fatigue crack initiation and propagation for particulate reinforced composites is facilitated with new Voronoi Cell Finite Element Method (VCFEM), considering the matrix-inclusion interfacial fatigue cracks, matrix fatigue cracks and crack closures. In the new element, all possible contacts on the crack edge is considered by contact seeking and remeshing methods, when the crack is closing under all possible changing loads. The fatigue crack initiates when the fatigue damage exceeds certain critical damage value, and fatigue crack propagation are simulated by gradual seeking crack propagating directions and new crack tips in a remeshing method.

The second example of Particle-reinforced metal-matrix composites with 20 elliptical inclusions shows that the VCFEM has considerable accuracy and high efficiency in dealing with the initiation and propagation of the fatigue crack. Good agreements are obtained between the results of VCFEM and the general finite element method, not given in this paper.

This kind of VCFEM method can predict functionally gradient material particles' interfacial crack accurately. The particles' size, topological structure, and interfacial deboning strength will influence FMES' mechanical behavior. With the interface cracking the overall stiffness of functionally gradient materials is gradually reduced.

Acknowledgements

The financial support by the National Natural Science Foundations of China (Nos. 11072092 and Nos. 11262007) is gratefully acknowledged.

References

[1] J. Zhang, and N. Katsube, A hybrid finite element method for heterogeneous materials with randomly dispersed rigid inclusions. Int J Numer Methods Eng, 38 (1995) 1635–1653.
[2] S. Ghosh, and S. N. Mukhopadhyay, Material based finite element analysis of heterogeneous media involving dirichlet tessellations. Comput Methods Appl Mech Eng, 104 (1993) 211–247.
[3] S. Ghosh, and S. Moorthy, Elastic-plastic analysis of arbitrary heterogeneous materials with the voronoi-cell finite-element method. Comput Methods Appl, 121 (1995) 373–409.
[4] S.Ghosh, Y. Ling, et al., Interfacial debonding analysis in multiple fiber reinforced composites. Mech mater, 32 (2000) 561–591.
[5] R. Guo, H. J. Shi and Z. H. Yao, Numerical simulation of thermo-mechanical fatigue properties for particulate reinforced composites. Acta Mechanica Sinica, 21(2) (2005) 160–168.
[6] R. Guo, H. J. Shi and Z. H. Yao, The modeling of interfacial debonding crack in particle reinforced composites using Voronoi cell finite element method. Comput Mech, 32(1-2) (2003) 52–59.